Wrinkling of Stimuloresponsive Surfaces: Mechanical Instability Coupled to Diffusion

Hugues Vandeparre and Pascal Damman*

Laboratoire Interfaces & Fluides Complexes, Centre d'Innovation et de Recherche en Matériaux Polymères, Université de Mons Hainaut, 20 Place du Parc, B-7000 Mons, Belgium

(Received 18 March 2008; revised manuscript received 17 July 2008; published 18 September 2008)

In this Letter, we propose a new mechanism to generate wrinkled patterns, based on the coupling between molecular diffusion and the buckling instability of rigid membranes ''glued'' on a polymer layer. The geometry of the diffusion front and the minimization of wrinkling energy conspire to generate various patterns of folds (e.g., parallel or radial folds, herringbone) and various dynamics (continuous or discrete). The diffusion process gives us the opportunity to study the stability of the various wrinkled patterns and to follow the creation or annihilation of topological defects.

DOI: 10.1103/PhysRevLett.101.124301 PACS numbers: 46.32.+x, 45.70.Qj, 62.23.St

Morphogenesis, i.e., the growth of forms and shapes, has fascinated scientists for centuries [1]. In nonequilibrium physics, a large effort was devoted to understanding the formation of regular patterns in dissipative systems [2,3]. More recently, it appears that self-organized structures could also be achieved at equilibrium. Once formed, the patterns are stable and do not require any continuous supply of energy. There is a great variety of physical and chemical systems that, at equilibrium, exhibit periodic patterns. For instance, stripes or ''bubbles'' could be observed in thin films of magnetic garnet, superconducting materials, block copolymers, liquid crystals, phospholipids, and ferrofluids (see [4] and references therein).

Wrinkling instability of compressed rigid membranes leads also to the formation of periodic patterns of stripes. Since the seminal papers of Tanaka *et al.* [5] and Bowden *et al.* [6], various systems were proposed to generate micrometric wrinkles via the application of compressive stresses to multilayers; see [7] for a recent review. In the limit of cylindrical symmetry, the formation of wrinkles in ''soft matter with hard skin'' [7] is satisfactorily described by physical models based on the elasticity of the hard skin and the stretching of the soft matter foundation [8,9]. The spatial layout of wrinkles can also be manipulated via the substrate topography [6], the rigidity of the topcoat [10], the confinement [11], or the adhesion at the substrate interface [12]. Understanding wrinkling processes also makes possible various applications such as the measurement of elastic modulus of ultrathin films [13], the design of microlens arrays [14], or silicon electronics on rubber substrates [15].

In the present Letter, we will focus on the formation of wrinkled patterns with complex morphologies, from the classical labyrinthine to the more sophisticated herringbone morphology, and on the role of defects in their stability. This last aspect, while very important in the study of patterns in block copolymers or liquid crystals [16], remains largely unexplored for wrinkling instability. A few attempts to study the stability of cylindrical patterns regarding compressive stresses were reported recently, together with phase diagrams describing the stability domains of the different morphologies [17–20]. By using a rather simple experimental setup, we have shown that wrinkling instability can be easily manipulated by solvent diffusion to produce various patterns, provided that stimuloresponsive multilayers are used. The growth dynamics of the patterns are controlled by the diffusion process, giving us the opportunity to follow the growth and annihilation of defects and to investigate the stability of the different morphologies.

The multilayers were prepared in two steps: (i) spin coating of high molecular weight atactic polystyrene solutions in toluene on bare silicon substrates (PS, $M_n \approx 10^6$ g/mol) to produce films with thicknesses ranging from 0.1 to 1 μm, and (ii) deposition of thin titanium (Ti) layers onto the polymer surface by thermal evaporation to thicknesses ranging from 10 to 20 nm. Wrinkling was then induced by immersing the multilayers in toluene vapors at room temperature in a homemade device allowing *in situ* optical microscopy observations. Toluene is a good solvent of PS that could swell the polymer layer below the Ti membrane. Linear and convex diffusion fronts were obtained from the edges of the sample and from the structural defects in the metal layer. Additionally, curved diffusion wave fronts appear when nonparallel linear fronts merge.

As shown in Fig. 1(a), PS/Ti multilayers put in contact with toluene vapors spontaneously form regular wrinkles that propagate together with the diffusion front. Strikingly, the resulting wrinkling patterns do not show the usual labyrinthine morphology [Fig. 1(b)] [6,12,21] but are clearly determined by the geometry of the diffusion process [Fig. 1(a)]. Parallel wrinkles are observed when the solvent diffuses from the edge yielding a linear front. Radial organization of wrinkles arises from pointlike diffusion starting at tiny holes randomly distributed in the thin metal layer (i.e., defects resulting from the deposition process). The wrinkles thus always grow preferentially

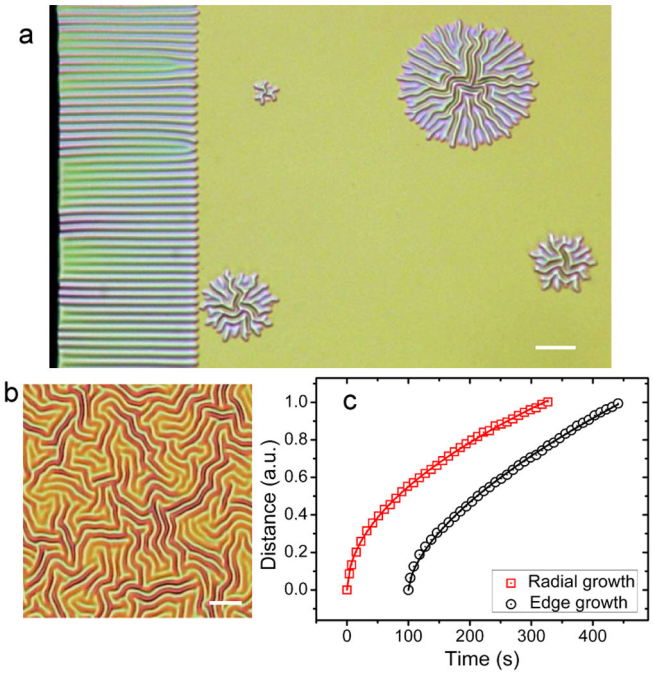

FIG. 1 (color online). (a) Optical micrographs of Ti/PS/SiOx wrinkled surfaces obtained with a 15-nm-thick metal layer and a 0.35 μm polymer layer after immersion in toluene vapors (scale bar 20 μm), (b) labyrinthine pattern of wrinkles obtained from a temperature jump [12] (scale bar 10 μm), and (c) dynamics of the wave-front position for radial and edge geometry. The experimental data were fitted according power laws ($D \propto t^{0.5\pm0.1}$). The curves were shifted along the time axis for clarity.

perpendicular to the wave front. The relevance of molecular diffusion in the observed phenomena is obviously supported by the dynamics of the process that follow the classical diffusive behavior, distance $\propto t^{1/2}$ [Fig. 1(c)].

Solvent diffusion is a rather uncommon way to wrinkle rigid membranes, usually compressive stresses are directly applied to the layer. We will first discuss the relation between diffusion and surface buckling. As previously reported, compressive stresses larger than a critical stress, $\sigma_c \sim E_m(h/H)(E_p/E_m)^{1/3}$ (where h, H, E_m, and E_p are the Ti and PS thicknesses, the elastic modulus of the rigid membrane, and the polymer, respectively), should be applied to induce wrinkling [8,9,12]. As a consequence, multilayers made up of low elastic modulus elastomers, such as polydimethylsiloxane (PDMS, $E_p \sim 10^5$ Pa), buckle with very small critical stresses. It was thus not surprising that metal surfaces deposited by thermal evaporation wrinkle during the deposition process [6]. The PDMS layer, thermally expanded during metal deposition, induces a compressive stress in the rigid membrane when cooled to ambient temperature. In contrast, replacing the elastomer with a high modulus glassy polymer, such as PS ($E_p \sim 10^9$ Pa), increases the critical stress by orders of magnitude. It could become so large that the thin metal surfaces, while stressed, remain perfectly flat after the thermal deposition. These stressed but flat titanium surfaces can thus be considered as ready to buckle membranes. The Ti/PS multilayers are, however, highly sensitive to chemical stimulation thanks to the polymer layer. Indeed, the diffusion of a good solvent, such as toluene, in PS leads to a drop of the glass transition temperature together with a drastic decrease of the elastic modulus (e.g., adding 15% of toluene is enough to obtain elastomeric PS at room temperature). To some extent, we could consider that solvent diffusion is equivalent to an increase of temperature for the PS layer. Since the formation of wrinkles is fully determined by the critical stress, strongly dependent on polymer elastic modulus, this diffusion process should trigger a transition from an unbuckled to a buckled state. As for thermal wrinkling, this transition leads to highly regular striped patterns with a well-defined wavelength [Fig. 2(a)]. Interestingly, we could see these structures as the mechanical counterpart of striped patterns of block copolymers, ferrofluids, or liquid crystals. In the framework of pattern formation at equilibrium [4], the distance between adjacent stripes, λ, should result from the competition between short-range and long-range interactions. For wrinkled surfaces, the "long-range repulsive interactions" between adjacent folds correspond to the bending of the rigid membrane, favoring large λ's, while "short-range attractive" ones could be related to the stretching of the polymer foundation, favoring small λ's.

The preferred wavelength can be easily obtained by minimizing the free energy penalty associated with the formation of wrinkles, involving the bending of the membrane, U_b, and the stretching of the polymer foundation, U_p. We consider cylindrical symmetry with a cosinusoidal deformation of the rigid membrane, $w(x) = A\cos(kx)$, where A and $k = 2\pi/\lambda$ are the amplitude of the deflection

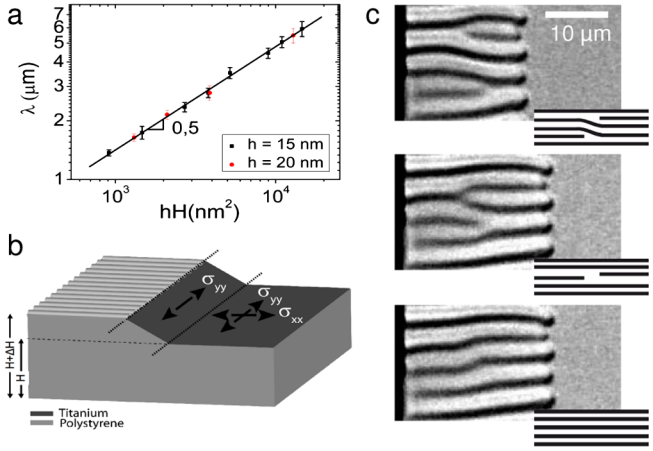

FIG. 2 (color online). (a) Evolution of the wavelength versus the product of metal and polymer thicknesses, hH for trilayers Ti/PS/SiOx immersed in toluene vapors (for edge geometry), (b) schematic representation of the stress field in the metal capping layer close to the wave front, and (c) successive optical microscopy images showing two oppositely oriented dislocations approaching and annihilating, in a growing striped pattern.

and the wave vector, respectively. The inextensibility condition implies that $A^2k^2 = \Delta_0$, Δ_0 being the imposed compressive strain. The bending energy is directly related to the curvature, C, via the relation $U_b = 1/\lambda \int \kappa C^2 dx$, where $C \sim (\partial^2 w/\partial x^2)$ and $\kappa = E_m h^3$ is the bending modulus, with h being the thickness of the metal membrane. Considering inextensibility, we obtain $U_b \sim E_m h^3 \Delta_0/\lambda^2$. The bending energy thus decreases when the wavelength increases (long-range repulsive interactions between wrinkles). The deformation of the polymer foundation can be related to the nondiagonal components of the strain tensor, $\epsilon_{xz} = 1/2(\partial u_x/\partial z + \partial u_z/\partial x)$, where u_x and u_z are the in-plane and out-of-plane displacements. The deformation energy of the foundation is thus given by $U_p \sim 1/\lambda E_p \int \epsilon_{xz}^2 dx dz \sim E_p A^2 \lambda^2/H^3$, where H is the thickness of the polymer. With inextensibility, the deformation energy becomes $U_p \sim E_p \Delta_0 \lambda^4/H^3$ and decreases when the wavelength decreases (short-range attractive interactions between folds). The minimization of the total free energy, $U_b + U_p$, gives the ideal distance between wrinkles $\lambda^* \sim (hH)^{1/2}(\frac{E_m}{E_p})^{1/6}$ in agreement with previous models [8,9,12] and the plot given in Fig. 2(a).

As previously reported, these wrinkled patterns can be obtained with various morphologies such as labyrinthine, herringbone, or uniaxial, depending on the preparation conditions [6,7,17,22]. In our experiments, however, the geometry of the diffusion wave front fully determines the layout of the wrinkles [Fig. 1(a)]. To explain this surprising observation, we should understand how the scalar field related to the solvent concentration could affect so strongly the elastic instabilities usually determined by the tensorial stress field. As demonstrated by the labyrinthine patterns of Fig. 1(b), the PS/Ti membranes are obviously subjected to an isotropic compressive stress field. Solvent diffusion thus plays the role of a symmetry breaking process that induces the growth of fully anisotropic patterns, linear or radial [Fig. 1(a)]. It is well known that the orientation of wrinkles is determined by the spatial distribution of compressive stresses; e.g., uniaxial stresses yield parallel wrinkles [22], while labyrinthine structures are observed for isotropic stresses. Before solvent diffusion, the film is initially flat, in a state of uniform stress ($\sigma_{xx} = \sigma_{yy}$). During solvent diffusion, the rigid membrane is stretched perpendicular to the wave front, due to the increase of film height associated with the swelling of the PS layer [Fig. 2(b)]. This uniaxial stretching induces a relaxation of the stress component perpendicular to the diffusion front and results in a locally anisotropic stress, at the origin of the symmetry breaking process ($\sigma_{xx} \ll \sigma_{yy}$).

The wrinkles induced by solvent diffusion should thus fit two geometric constraints: (i) the distance between adjacent wrinkles, λ, should be equal to the theoretical wavelength λ^* that minimizes the elastic energy, and (ii) the wrinkles should be perpendicular to the diffusion wave front.

These two constraints can be easily fulfilled when the solvent diffuses from the edge (linear geometry). Indeed, the wrinkles are aligned perpendicularly to the edge and adopt the theoretical wavelength as illustrated by the evolution of λ with the metal and polymer thicknesses, $\lambda \propto (hH)^{1/2}$ [Fig. 2(a)]. However, the striped patterns of wrinkles also reveal topological defects such as elementary dislocations and disclinations similar to those observed in block copolymer thin films [16]. Obviously, dislocations [Fig. 1(a)] leads to a local perturbation of the wrinkles' interdistance and are therefore energetically unfavorable. As shown in Fig. 2(c), opposite dislocations thus attract and annihilate to produce patterns free of topological defects.

For buckled domains with pointlike diffusion, the radial symmetry is incompatible with the two constraints that should impose an interdistance as close as possible to the ideal wavelength λ^* together with a splaying fanlike morphology (wrinkles should be perpendicular to the wave front). These constraints produce an astonishing growth process described by a switchback dynamics that could be related to a continuous creation of dislocations (Fig. 3). In fact, the radial symmetry imposes a continuous increase of the wrinkles interdistance, λ, whereas the fold number should be an integer. The number of wrinkles around the circular edge thus remains constant, until a new fold could be intercalated in the rigid membrane, creating a new dislocation. In other words, the energetic penalty associated with the dislocation becomes lower than the energy related to the increase of wrinkles interdistance. We could easily rationalize these observations by introducing an effective number of folds, N_{eff}, and considering that the perimeter is given by $P = N\lambda = N_{\text{eff}}\lambda^*$, where N and N_{eff} are the true (integer) number of folds and an effective (real)

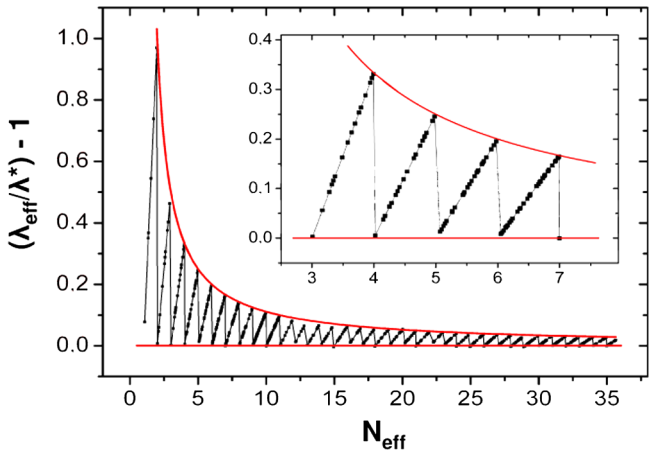

FIG. 3 (color online). Analysis of the wrinkling dynamics for a Ti(15 nm)/PS(0.35 μm)/SiOx trilayer immersed in toluene vapors, for pointlike diffusion. Zigzag decrease of the normalized wavelength, $\frac{\lambda}{\lambda^*} - 1$ with the effective number of folds, $N_{\text{eff}} = 2\pi r/\lambda^*$ (see text). The envelope determined by the maxima follows the $1/N$ law (solid line). The inset shows an excerpt of the curve.

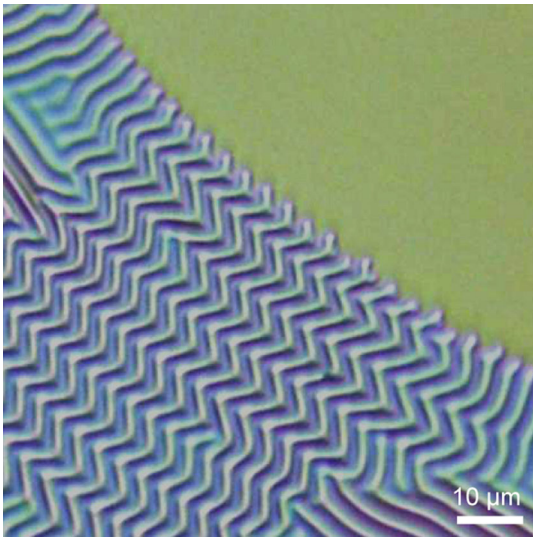

FIG. 4 (color online). Optical micrograph of Ti/PS/SiOx wrinkled surfaces recorded during toluene diffusion. The slightly curved wave front induces the formation of a herringbone morphology. Scale bar is 10 μm.

number of folds corresponding to the observed mean interdistance, λ, and the ideal wavelength, λ^*, respectively. We thus get the relation $\lambda/\lambda^* - 1 = (N_{\text{eff}} - N)/N$ that fits the evolution of the experimental data (Fig. 3). The interdistance increases linearly and when N_{eff} becomes an integer, the system intercalates a new fold (a dislocation), going to the next integer value of the total number of folds, $N = N + 1$. The process is iterative and finally yields the switchback shape of the curve. Since the addition of one fold occurs when $N_{\text{eff}} = N + 1$, the envelope curve should be given by the simple relation $\lambda/\lambda^* - 1 = 1/N$ (see Fig. 3).

In addition to the parallel stripes and radial wrinkled patterns, more complex geometry could be observed. As shown in Fig. 4, curved wave fronts are unstable and spontaneously transform in the herringbone morphology. These observations obviously confirm that, as expected, the compressive stresses in the Ti membrane are really isotropic. The equilibrium morphology should thus correspond to the most stable labyrinthine or herringbone patterns, the systems selecting one or the other from the ''stress release history'' [19,20]. But, these observations also demonstrate that the transition from one morphology to the other requires a nucleation event. A pattern of parallel wrinkles remains perfectly stable unless some imperfections, e.g., curvature, nucleate the energetically more stable herringbone morphology. As for first order transitions, it seems there is an energy barrier to transform linear parallel wrinkles to undulated patterns. We suggest that this energy barrier could be related to the nonzero Gaussian curvature that appears inevitably when a cylinder is bent. The influence of Gaussian curvatures on stress focusing in crumpled membranes was recently discussed in Ref. [23].

The stability of wrinkled patterns obtained from the elastic instability of rigid membranes not only depends on the applied compressive stresses but also on the imperfections of the patterns.

The authors thank J. Léopoldès for the suggestion to induce wrinkling by solvent immersion, and C. Gay, A. Boudaoud, and B. Audoly for stimulating discussions. The Belgian National Fund for Scientific Research (FNRS) and the Walloon region (research project CORRONET) are acknowledged for financial support.

*pascal.damman@umh.ac.be

[1] P. Ball, *The Self-Made Tapestry: Pattern Formation in Nature* (Oxford University Press, New York, 1999).
[2] C. Bowman and A. C. Newell, Rev. Mod. Phys. **70**, 289 (1998).
[3] M. C. Cross and P. C. Hohenberg, Rev. Mod. Phys. **65**, 851 (1993).
[4] M. Seul and D. Andelman, Science **267**, 476 (1995).
[5] T. Tanaka, S. T. Sun, Y. Hirokawa, S. Katayama, J. Kucera, Y. Hirose, and T. Amiya, Nature (London) **325**, 796 (1987).
[6] N. Bowden, S. Britain, A. G. Evans, J. W. Hutchinson, and G. M. Whitesides, Nature (London) **393**, 146 (1998).
[7] J. Genzer and J. Groenewold, Soft Mater. **2**, 310 (2006).
[8] E. Cerda and L. Mahadevan, Phys. Rev. Lett. **90**, 074302 (2003).
[9] Z. Y. Huang, W. Hong, and Z. Suo, J. Mech. Phys. Solids **53**, 2101 (2005).
[10] W. T. S. Huck, N. Bowden, P. Onck, T. Pardoen, J. W. Hutchinson, and G. M. Whitesides, Langmuir **16**, 3497 (2000).
[11] P. J. Yoo, K. Y. Suh, S. Y. Park, and H. H. Lee, Adv. Mater. **14**, 1383 (2002).
[12] H. Vandeparre, J. Leopoldes, C. Poulard, S. Desprez, G. Derue, C. Gay, and P. Damman, Phys. Rev. Lett. **99**, 188302 (2007).
[13] C. M. Stafford, C. Harrison, K. L. Beers, A. Karim, E. J. Amis, M. R. Vanlandingam, H.-C. Kim, W. Volksen, R. D. Miller, and E. E. Simony, Nature Mater. **3**, 545 (2004).
[14] E. P. Chan and A. J. Crosby, Adv. Mater. **18**, 3238 (2006).
[15] D.-Y. Khang, H. Jiang, Y. Huang, and J. A. Rogers, Science **311**, 208 (2006).
[16] C. Harrison, Z. Cheng, S. Sethuraman, D. A. Huse, P. M. Chaikin, D. A. Vega, J. M. Sebastian, R. A. Register, and D. H. Adamson, Phys. Rev. E **66**, 011706 (2002).
[17] X. Chen and J. W. Hutchinson, J. Appl. Mech. **71**, 597 (2004).
[18] L. Mahadevan and S. Rica, Science **307**, 1740 (2005).
[19] T. Ohzono and M. Shimomura, Phys. Rev. E **73**, 040601 (R) (2006).
[20] B. Audoly and A. Boudaoud, J. Mech. Phys. Solids **56**, 2401 (2008).
[21] P. J. Yoo, K. Y. Suh, H. Kang, and H. H. Lee, Phys. Rev. Lett. **93**, 034301 (2004).
[22] K. Efimenko, M. Rackaitis, E. Manias, A. Vaziri, L. Mahadevan, and J. Genzer, Nature Mater. **4**, 293 (2005).
[23] T. A. Witten, Rev. Mod. Phys. **79**, 643 (2007).